

An investigation of Knoevenagel condensation reaction in microreactors using a new zeolite catalyst

Xiongfeng Zhang^{a,1}, Emily Sau Man Lai^a, Rosa Martin-Aranda^b, King Lun Yeung^{a,*}

^a Department of Chemical Engineering, The Hong Kong University of Science and Technology, Clear Water Bay, Kowloon, Hong Kong (SAR), PR China

^b Departamento de Química Inorgánica y Química Técnica, Universidad Nacional de Educación a Distancia, C/ Senda del Rey, 9, 28040-Madrid, Spain

Received 27 October 2003; received in revised form 27 October 2003; accepted 28 October 2003

Abstract

New basic zeolite catalysts obtained by grafting amino groups onto NaX and CsNaX zeolites exhibit excellent catalytic activities for Knoevenagel condensation reaction between benzaldehyde and ethyl cyanoacetate (ECA), ethyl acetoacetate (EAA) and diethyl malonate (DEM). The CsNaX-NH₂ catalyst also displays higher conversion compared to aminopropylated MCM-41. Knoevenagel condensation reaction in a CsNaX zeolite microreactor performed better than the traditional packed bed reactor (PBR) with an order of magnitude higher productivity (i.e. moles ethyl 2-cyano-3 phenylacrylate produced per hour for each gram catalyst). A nearly fourfold increase in reaction conversion was obtained for the microreactor when CsNaX-NH₂ catalyst was used. A membrane microreactor was obtained by incorporating a water-selective, NaA membrane to the multi-channel microreactor. The selective removal of water byproduct during the reaction led to a 25% improvement in reaction conversion for both catalysts.

© 2003 Elsevier B.V. All rights reserved.

Keywords: Knoevenagel condensation; Zeolite; Microporous and mesoporous

1. Introduction

The potential use of microporous and mesoporous base catalysts in fine chemical production is enormous [1–3]. Base-catalysed condensation and addition reactions are some of the important reaction steps employed for building large and complex molecules that characterizes many of the fine chemicals and pharmaceutical products. Other reactions such as trans-esterification and isomerization have applications in food and cosmetic industries [4,5]. Replacing the liquid organic bases (e.g. piperidine), alkali metal hydroxides and alkoxides with solid base catalysts can lead to cleaner productions. These heterogeneous catalysts are known to suppress side reactions that include self-condensation and oligomerization, resulting in better selectivity and product yield. This means cost and energy savings for the downstream separation and purification of the product. It also avoids the complex neutralization and

separation steps needed to recover the homogeneous base catalysts from the reaction mixture. The recovered solid catalysts can be readily regenerated for further use.

The Knoevenagel condensations between carbonylic compounds and methylene malonic esters produce several important key products that include nitriles used in anionic polymerization and the α,β -unsaturated ester intermediates employed in the synthesis of several therapeutic drugs (e.g. nifendipine and nitrendipine) and pharmacological products (e.g. calcium channel blockers and antihypertensives). Alkali metal hydroxides (e.g. NaOH and KOH), pyridine and piperidine are the traditional catalysts used in these reactions. However, basic zeolites such as Cs-exchanged NaX (CsNaX) and GeX, as well as cesium and cesium-lanthanum impregnated mesoporous MCM-41 are also able to catalyze the Knoevenagel condensation under mild reaction conditions [6–9]. It has been shown that nitridation of zeolite materials with ammonia produces more basic catalysts than the ion-exchanged zeolites [10]. This process replaces the hydroxyl groups in the zeolite with amino groups, which is then converted into active nitrogen-bearing basic sites after high temperature treatment (i.e. usually in excess of 1073 K). This work investigates the possibility of achieving the same

* Corresponding author. Tel.: +852-2358-7123; fax: +852-2358-0054.

E-mail address: kekyeung@ust.hk (K.L. Yeung).

¹ Present address: Department of Chemical Engineering, Dalian University of Technology, Dalian, PR China.

catalyst improvement by grafting aminopropyl groups onto the NaX and CsNaX zeolites. This procedure is simple and does not require high temperature treatments.

Recently, it has been successfully shown that zeolite and molecular sieves materials could be incorporated as catalyst [11–13], membrane [11,14] and structural material [15,16] in miniature chemical devices such as microreactors and microseparators. Miniaturization benefits both reaction and separation by improving mass and heat transfer rates through increased interfacial area and shorter diffusion path length [17]. Indeed, reactions conducted in zeolite microreactors were reported to have better selectivity and higher product yield [12,13,18]. Also, zeolite micromembranes displayed excellent selectivity and permeation flux for gas permeation [14], liquid pervaporation [19] and liquid-liquid separation [20]. The enhanced reaction and separation in chemical microsystems mean better reactant utilization and less waste generation leading to a cleaner chemical synthesis. Besides catalyst improvement, this work also investigates the advantage of using zeolite microreactor and zeolite membrane microreactor for the Knoevenagel condensation reaction. The reaction between benzaldehyde and ethyl cyanoacetate was chosen as the test reaction for this study, because of the large body of literature data available for this reaction system.

2. Experimental

2.1. Catalyst preparation and characterization

The Faujasite Y and X zeolite powders were purchased from Aldrich chemicals. The zeolite powder was ground, sieved and calcined prior to use, in order to obtain a uniform catalyst powder free of moisture and adsorbed organic contaminants. The CsNaX was prepared by ion exchange of NaX powder with 0.5 M cesium chloride solution at 353 K for 6 h. This procedure was repeated three times to obtain a desired Cs/Si loading of 0.32. An active CsNaX catalyst was obtained after pretreatment in air at 673 K for 4 h. The NaX-NH₂ and CsNaX-NH₂ were prepared by grafting 3-aminopropyl-trimethoxysilane (APTS) onto NaX and CsNaX zeolites, respectively. Five grams of zeolite powders were refluxed in a dry toluene solution (250 ml) containing 18 ml of APTS (97%, Aldrich Chemicals) at 383 K for 18 h. The catalysts were recovered by filtration after washing in dry toluene, distilled deionized (DDI) water and acetonitrile. The powders were dried in an oven at 373 K and stored for later use. The structure and composition of the zeolite catalysts were analyzed by electron microscopy (SEM, JEOL 6300), X-ray diffraction (XRD, Philip PW 1030), X-ray fluorescence spectroscopy (XRF, JEOL JSX-3201Z) and X-ray photoelectron spectroscopy (XPS, Physical Electronics, PHI 5600). The amount of grafted organic amino groups was measured by thermal gravimetric and differential thermal analyses (TGA/DTA, Setaram).

The zeolite catalysts were tested for Knoevenagel condensation reactions between benzaldehyde (99%, RDH) and (a) ethyl cyanoacetate (ECA, >98%, Aldrich), (b) ethyl acetoacetate (EAA, 99%, Aldrich) and (c) diethyl malonate (DEM, 99%, Aldrich). A stoichiometric mixture containing 14 m moles of benzaldehyde (99%, RDH) and 14 m moles of malonic ester derivative (e.g. ECA, EAA and DEM) was placed in a batch reactor (i.e. 10 ml flask) and heated to the reaction temperature under constant stirring. 1 wt.% of catalyst powders (0.031 g) was added to the reactant mixture to initiate the reaction. Solvent was not used and the reaction was conducted under nitrogen atmosphere to prevent the formation of byproducts (e.g. benzoic acid). Samples were taken periodically for analysis by gas chromatography to monitor the reaction and to obtain the kinetic data. The gas chromatograph (GC, HP 5890) was equipped with a 60-m phenylsilicone capillary column (Alltech) and a flame ionisation detector. The stirring rate was kept at 1000 rpm to eliminate external mass transfer resistance. The small particle size of the catalyst ensured that the internal diffusion resistance was low.

2.2. Design and fabrication of a microreactor

Although most microreactors were made from silicon substrate, stainless steel was chosen for this study for its low cost, machinability and better compatibility with most reaction systems. Our microreactor consisted of a multi-channel plate and a stainless steel housing as shown in Fig. 1. The design emphasized on flexibility and ease of use. The separate design and fabrication of the micro-component architecture contained in the plate enabled the rapid testing of different microreactor architectures. The housing unit provided a convenient interface between the microreactor and the macroscale laboratory environment. It contained the inlet, outlet, vacuum and sensor feedthroughs, as well as a window for direct observation of the reaction by microscopy and spectroscopy.

2.2.1. Multi-channel, membrane-catalyst plate

A multi-channel plate (Fig. 1a) was made by cutting microchannels onto a 25 mm × 25 mm porous stainless steel plate (0.2 μm pores) purchased from Mott metallurgical corporation. Thirty-five microchannels, each 300 μm wide, 600 μm deep and 25 mm long, were cut into the stainless steel plate using electro-discharge micromachining (AGIE Wirecut 120). This method prevented the collapse of the pores during the machining of the microchannels. After the multi-channel plate was cleaned with detergent and water to remove dirt and contaminants, it was sonified in dilute nitric acid solution (69%, BDH) followed by ethanol and acetone rinses to remove oxide layers before it was dried in an oven at 348 K.

A layer of hydrophilic NaA zeolite membrane was grown on the back of the multi-channel plate by pre-seeding with

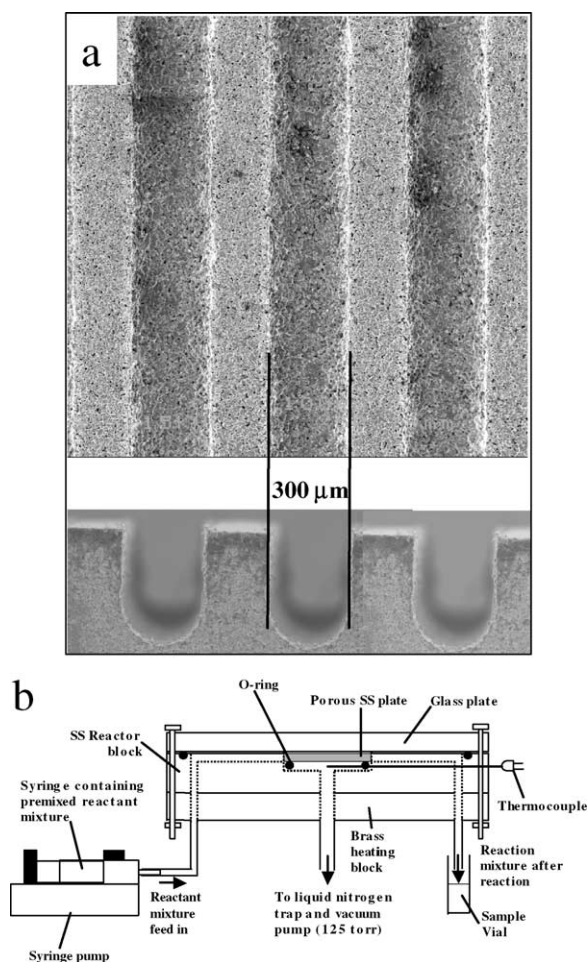


Fig. 1. (a) Scanning electron microscope pictures of the microchannels cut onto a porous stainless steel. (b) Schematic diagram of the multi-channel microreactor set-up.

NaA zeolite seeds (150 ± 20 nm) followed by regrowth in a synthesis solution containing a molar composition of $5\text{SiO}_2:\text{Al}_2\text{O}_3:52\text{Na}_2\text{O}:3750\text{H}_2\text{O}$. The silica precursor was obtained by hydrolysis of tetraethyl orthosilicate (98%, Aldrich), while sodium aluminate purchased from Riedel-de Haën provided the alumina source. The pH of the synthesis mixture was adjusted using sodium hydroxide (99%, Riedel-de Haën). The synthesis was conducted in an autoclave vessel at 373 K for 10 h. After membrane deposition, the plate was rinsed with DDI water and dried prior to weighing and inspection with an optical microscope to determine the amount and coverage of zeolite deposit. The synthesis was repeated three times to obtain a defect-free NaA membrane. The final membrane was examined with XRD and SEM (JEOL 6300) to determine the membrane structure.

CsNaX and CsNaX-NH_2 catalysts were deposited onto the microchannels by the following procedures. A thin layer of polydiallyldimethyl ammonium chloride (PDAMAC, MW = 200,000–350,000, Aldrich) was coated onto the mi-

crochannel from a 20 wt.% PDAMAC solution. The coating was applied using a brush and was blown dried with compressed air. The multi-channel plate was pressed face down against a clean glass plate. Two milliliter of dilute catalyst suspension (1 wt.%) in water was placed near the channel openings and drawn into the microchannel with the aid of a light suction. The negatively charged zeolite particles were deposited onto the positively charged PDAMAC-coated microchannel walls. After drying at room temperature, the plate was heat treated at 523 K for 12 h to obtain a good catalyst adhesion on the microchannels. The amount of deposited catalyst was determined from the weight difference between the coated and uncoated multi-channel plate. Visual inspection using optical microscope and detailed imaging by SEM provided information on the catalyst coverage within the microchannels.

2.2.2. Microreactor housing

The microreactor housing was machined from a single block of stainless steel (SS-316) plate and consisted of a receptacle for the multi-channel plate, inlet and outlet ports for the reaction fluid, and feedthroughs for sensors and vacuum (Fig. 1b). The fluid ports and feedthroughs are located underneath the housing unit. Liquid reactants fed by a syringe pump (Kd Scientific) entered the inlet port into a narrow rectangular channel (1 mm \times 25 mm) formed between the housing and the Pyrex glass cover. The liquid was evenly distributed along the width of the channel by a set of baffles before it reached the multi-channel plate. This ensured that the liquid flowed uniformly through each of the microchannels. A similar set of baffles guided the liquid leaving the multi-channel plate to the exit port, where it was collected in sealed vials at room temperature and kept for later analysis. Located beneath the receptacle holding the multi-channel plate was the vacuum port connected to a pressure gauge and a vacuum pump (Barnant Company). A liquid nitrogen trap was used to condense and collect the vapor that pervaporated across the zeolite membrane. Thermocouples were inserted at different locations to measure the temperature of the entering and exiting fluid and that of the multi-channel plate. Heat was provided by a brass heating block equipped with a pair of heating rod controlled by a temperature controller (Rex-C100, RKC).

2.3. Knoevenagel condensation in microreactors

2.3.1. Zeolite membrane pervaporation

Prior to the reaction experiments, the multi-channel, membrane-catalyst plate was tested for the pervaporation of water/benzaldehyde mixtures. The liquid solution was fed at a flow rate of 1 ml/h and the membrane pervaporation was conducted at a temperature of 373 K and vacuum pressure of 125 Torr. The retentate was cooled at room temperature and collected in a sample vial, whereas the permeate stream was condensed and collected in a liquid nitrogen trap. The

liquids collected from the retentate and permeate were first weighed, before analysis by gas chromatography. The permeate flux (P) in $\text{Kg h}^{-1} \text{m}^{-2}$ was calculated from:

$$P = \frac{P_M}{A} \quad (1)$$

where P_M is the average mass flow rate across the membrane in kg h^{-1} and A is the membrane area of $6.25 \times 10^{-4} \text{m}^2$. The selectivity of the membrane separation (α) was calculated from the composition of the liquids collected from the retentate and permeate.

$$\alpha = \frac{Y_{\text{H}_2\text{O}}/Y_{\text{organics}}}{X_{\text{H}_2\text{O}}/X_{\text{organics}}} \quad (2)$$

where Y_i and X_i are weight fraction of component i in the permeate and retentate, respectively.

2.3.2. Knoevenagel condensation reaction

Equimolar solution of benzaldehyde and ethyl cyanoacetate were mixed in a nitrogen hood to prevent the formation of benzoic acid. A 25 ml syringe (Hamilton) was rinsed and filled with the reactant solution. The preheated reactor (i.e. 373 K) was manually filled with the reactant solution, taking care that no bubbles were formed during the process. Once the reactor was filled, the syringe was transferred to the syringe pump and the liquid was fed at a fixed rate (i.e. 0.2–12 ml/h). Samples were collected only after two hours of the reaction. Two sets of experiments were conducted each day. At the start of the experiment, the multi-channel plate was run as a microreactor with the permeate vacuum closed, and the reaction solution was collected from the reactor outlet at fixed intervals to determine steady-state condition. In the second experiment, the vacuum was turned on and the multi-channel plate was operated as a membrane microreactor. Samples were obtained from both the reactor and permeate outlets.

After filtering the quenched samples, 10 μl of the reaction solution was diluted with 1 ml of *tert*-butyl methyl ether (MTBE, 99.8%, Fluka) and injected into the gas chromatograph. Three GC measurements were made for each sample and the concentration of the reactants and products were determined from a calibration curve prepared from standard solutions containing known quantities of benzaldehyde, ethyl cyanoacetate and ethyl 2-cyano-3 phenylacrylate (98%, TCI). Samples collected from the permeate outlet were also analyzed by TOC analyzer (TOC 500, Shimadzu) after dilution with DDI water to determine the amount of organic carbon. The benzaldehyde conversion and ethyl 2-cyano-3-phenylacrylate yield along with the permeate flux (P) and membrane separation (α) were used to evaluate the microreactor and membrane microreactor performance.

3. Results and discussion

3.1. Zeolite catalysts for Knoevenagel condensation reaction

The Faujasite zeolite powders obtained after crushing, sieving and calcination had an average particle size of 2 μm and formed aggregate clusters of about 6 μm in diameter. Analyses by electron microscopy revealed mostly spherical particles with poorly formed facets. Despite the lack of particles with the characteristic bipyramidal shape of Faujasite crystals, X-ray diffraction data indicated the absence of impurities. There was no detectable change in the size and shape of zeolite particles after ion exchange with cesium (i.e. CsNaX, CsNaX-NH₂) and addition of aminopropyl group (i.e. NaX-NH₂, CsNaX-NH₂). Fig. 2 displays the X-ray diffraction patterns of the original and modified NaX zeolites. The calcined NaX powder displays the characteristic diffraction pattern of dehydrated NaX zeolite [21]. Ion exchange with CsCl₂ led to weaker peak intensities and disappearance of (3 3 1) and (4 4 0) diffraction lines. The presence of new diffraction peaks at $2\theta = 12, 25.5,$ and 27.5 that had been assigned to Cs-exchanged NaX [22] is a strong evidence of a successful catalyst preparation. Grafting aminopropyl groups onto NaX and CsNaX also resulted in lower X-ray peak intensities, but no new diffraction peaks appeared in these samples (Fig. 2).

Elemental analyses of the zeolite samples by XPS and XRF detected a decrease in the sodium content of the zeolite and the appearance of cesium after the ion exchange (Table 1). Over 60% of the original sodium in NaX zeolite was exchanged for cesium (i.e. Cs/(Cs + Na) = 0.60). A slight decrease in the surface area (i.e. 430–400 m^2/g) was observed after cesium ion exchange. Both Rodriguez et al. [23] and Lasperas et al. [24] also made similar observations.

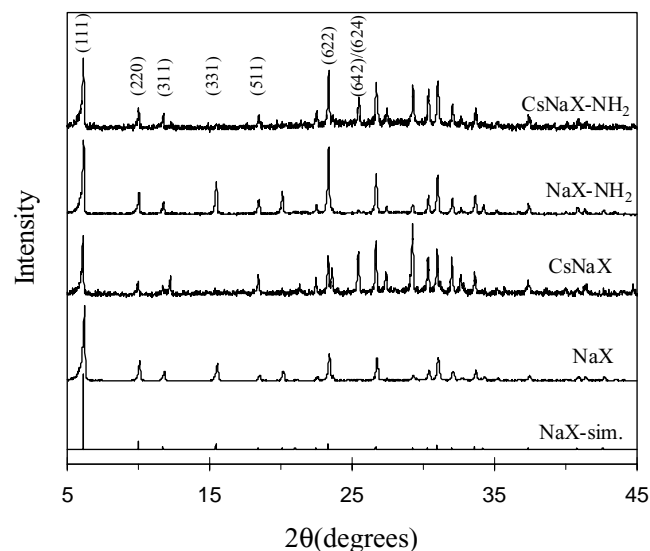


Fig. 2. X-ray diffraction pattern of zeolite catalysts tested for Knoevenagel condensation reaction.

Table 1
Physical and chemical properties of the zeolite catalysts

| Physical and chemical properties | NaY | NaX | CsNaX | NaX-NH ₂ | CsNaX-NH ₂ | OMS-NH ₂ |
|---|-------|-------|-------------|---------------------|-----------------------|---------------------|
| Average particle size ^a (μm) | 2.3 | 2.1 | 1.9 | 2.1 | 1.8 | 1.2 |
| BET ^b surface area (m ² /g) | 480 | 430 | 400 | 80 | 200 | 750 |
| Cs/Si ratio ^c , bulk (surface) | 0 (0) | 0 (0) | 0.32 (0.20) | 0 (0) | 0.24 (0.10) | 0 (0) |
| Cs/(Na + Cs) ratio ^c , bulk (surface) | 0 (0) | 0 (0) | 0.60 (0.63) | 0 (0) | 0.60 (0.67) | 0 (0) |
| N/Si ratio ^c , bulk (surface) | 0 (0) | 0 (0) | 0.10 (0) | 3.0 (0.21) | 3.1 (0.29) | – |
| Amino groups ^d (mmole/g) | 0 | 0 | 0 | 1.4 | 1.2 | 2.2 |

^a The average particle size was measured from the scanning electron microscope pictures.

^b The BET surface area was obtained after the zeolite sample was calcined in air at 773 K for 8 h to burn away the organic groups.

^c The bulk and surface compositions were calculated from the XRF and XPS data, respectively.

^d The amount of organic moieties on the zeolites was determined from the TGA/DTA data.

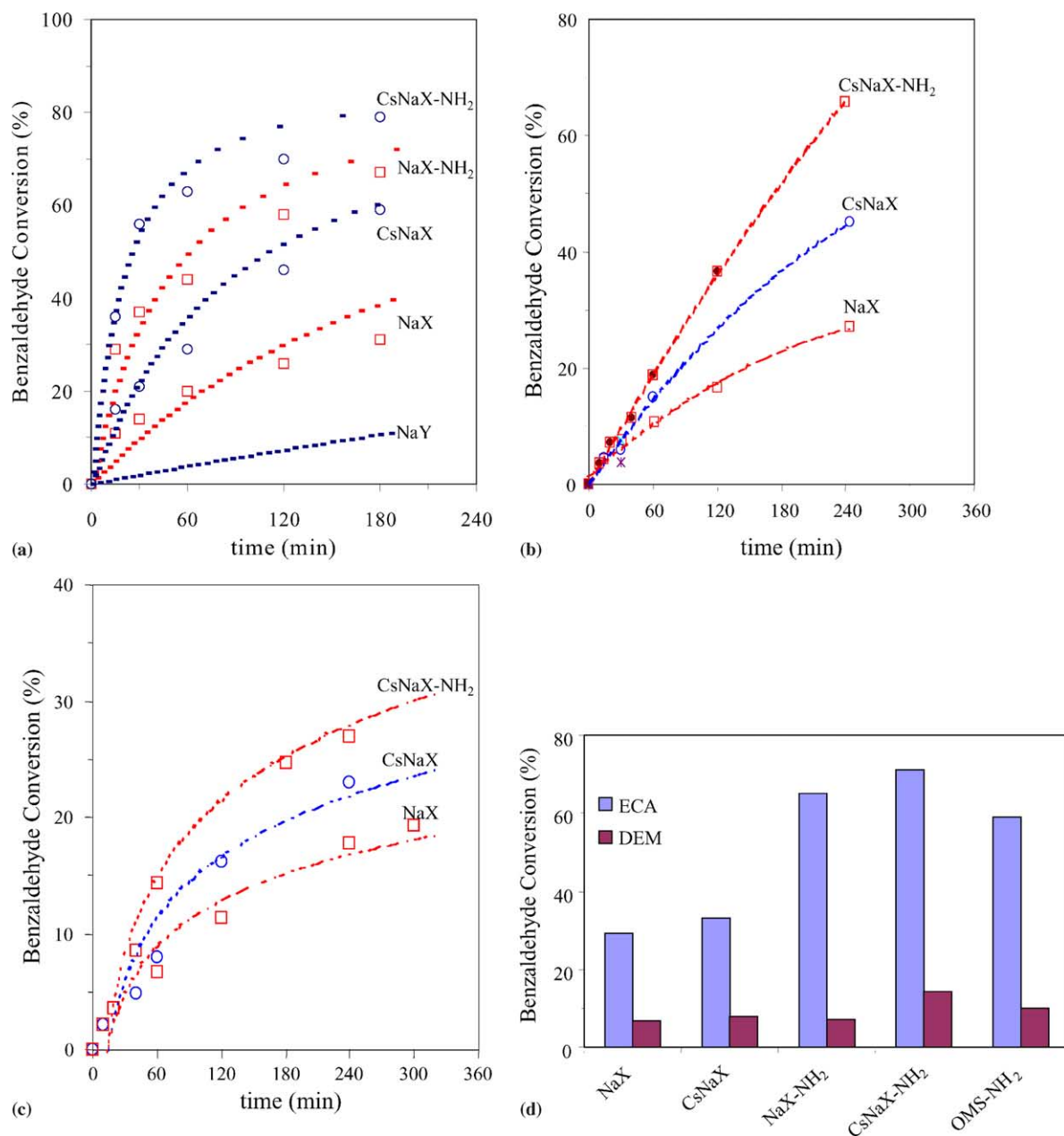
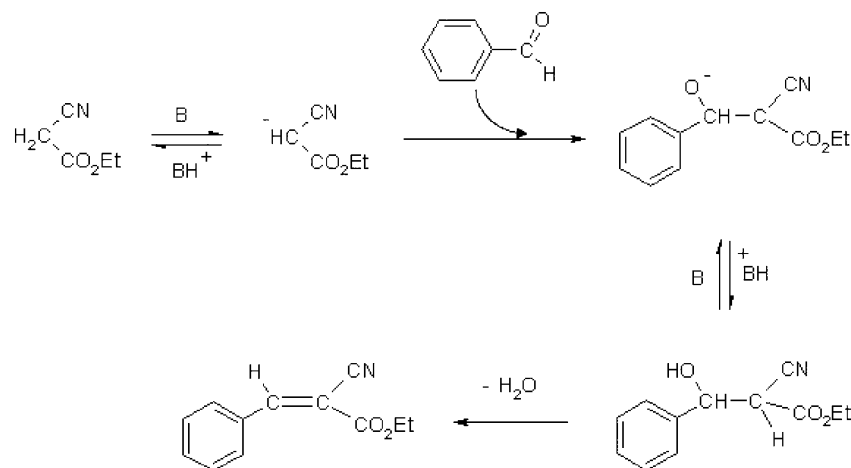


Fig. 3. Benzaldehyde conversion in a batch reactor as a function of reaction time for (a) ethyl cyanoacetate at 363 K (Note: symbol—experimental data, dashed line—model calculation), (b) ethyl acetoacetate at 393 K and (c) diethyl malonate at 393 K. (d) Benzaldehyde conversion for reactions with ECA and DEM conducted at 393 K, 1 wt.% catalyst loading and reaction time of 60 min. Please note the line in Fig. 3b and c were drawn only to guide the eyes.



Scheme 1. Classical reaction scheme for solid-base catalyzed Knoevenagel condensation reaction.

It was suggested that the loss of surface area was caused by breakage of Si–O–Si bonds leading to pore collapse [8], but it was also possible that the smaller surface area was due to the restricted access to the zeolite pore channel caused by the presence of large cesium counterions [25]. The amount of grafted organic amino groups was found by thermal gravimetric and differential thermal analyses (TGA/DTA, Setaram) to be 1.4 and 1.2 m moles/g for NaX-NH₂ and CsNaX-NH₂, respectively. A decrease in the Na/Si signal was observed by XPS and XRF after the RNH₂ groups were grafted onto the zeolites (Table 1). In addition, the catalyst surface areas were also smaller than the original NaX and CsNaX zeolite precursors. Nitrogen physisorption and TGA/DTA analyses suggested that for NaX-NH₂ most of the aminopropyls resided inside the zeolite pores. This may explain the small BET surface area measured for this sample.

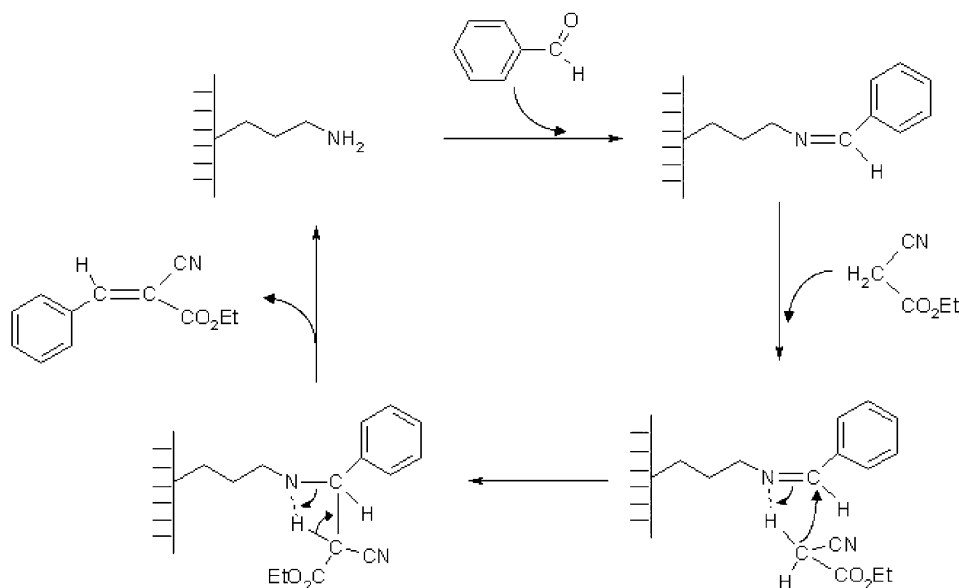
Fig. 3a plots the benzaldehyde conversion as a function of reaction time for NaY, NaX, CsNaX, NaX-NH₂ and CsNaX-NH₂ catalysts. Ethyl 2-cyano-3-phenylacrylate was the only product obtained using these catalysts. The trace amount of benzoic acid detected in the reaction mixture originated as impurity from the benzaldehyde reactant. The classical reaction scheme for Knoevenagel condensation reaction is shown in Scheme 1. A second-order reversible kinetic rate expression was derived assuming that the addition of the enolate anion onto the benzaldehyde is the rate-limiting step in the reaction. The enolate anion is formed when the catalyst removes a proton from the methylenic group of the ethyl cyanoacetate. Its addition to the benzaldehyde creates a metastable adduct that rapidly transform into the final condensation product with the release of a hydroxyl anion. The integrated form of the rate equation for the equimolar mixture is,

$$\ln \frac{X_E - (2X_E - 1)X}{X_E - X} = 2k_1[S_0](X_E^{-1} - 1)C_0t \quad (3)$$

where X_E is the equilibrium benzaldehyde conversion at the reaction temperature, X the conversion of benzaldehyde, k_1

reaction rate constant, S_0 the concentration of basic sites, C_0 the initial concentration of benzaldehyde in the reaction mixture and t is the reaction time. This reaction rate expression is also consistent with the proposed reaction scheme for Knoevenagel condensation reaction catalyzed by surface grafted primary amines (Scheme 2) [26]. Fig. 3a shows that there is a good fit between model and experiment. The value of $k_1[S_0]$ gave a qualitative measure of the number and strength of the basic sites created by the different preparation procedures. The NaX zeolite is four times more active than NaY for this condensation reaction. Ion exchange of NaX zeolite with cesium (i.e. CsNaX) increases the catalyst activity by threefold, but this is less when compared to NaX-NH₂, which exhibits fivefold increase in the activity compared to the NaX. The activity of CsNaX can be further improved by grafting 1.4 m mole/g of aminopropyls onto the catalyst. The CsNaX-NH₂ activity is three times higher than CsNaX and is indeed more active than the GeX [6].

The reactivity of NaX, CsNaX and CsNaX-NH₂ catalysts was also tested for the Knoevenagel condensation of benzaldehyde with ethyl acetoacetate (Fig. 3b) and diethyl malonate (Fig. 3c). The reactions were conducted at 393 K using 1 wt.% catalyst loading. These reactions were carried out to probe the basicity of the active sites [27] created by grafting aminopropyl groups onto CsNaX catalyst. Fig. 3b and c show that CsNaX-NH₂ has the highest reactivity followed by CsNaX with the unmodified NaX having the lowest reaction conversion. Comparison was also made between CsNaX-NH₂ and aminopropylated MCM-41 (OMS-NH₂). The mesoporous silica catalyst contained 2.2 m mole/g of grafted amino groups and had a surface area of about 750 m²/g [28]. This gave OMS-NH₂ a surface concentration of 1.7 amino groups per nm² (cf. Table 1). Fig. 3d summarizes the benzaldehyde conversion after 60 min of reactions. For the reaction between benzaldehyde and ethyl cyanoacetate, the conversion of CsNaX-NH₂ > NaX-NH₂ > OMS-NH₂ > CsNaX > NaX. Indeed, the initial reaction rate for CsNaX-NH₂ ($R_0 = 0.74 \text{ mol}^1 \text{ g}_{\text{cat}}^{-1} \text{ h}^{-1}$)



Scheme 2. Proposed reaction scheme for Knoevenagel condensation reaction catalyzed by surface grafted organic amines [29].

was larger than the OMS-NH₂ ($R_0 = 0.62 \text{ mol}^1 \text{ g}_{\text{cat}}^{-1} \text{ h}^{-1}$). Similarly, the conversion of CsNaX-NH₂ > OMS-NH₂ > CsNaX > NaX-NH₂ ~ NaX for the reaction of benzaldehyde and diethyl malonate. This clearly showed that the new CsNaX-NH₂ catalyst is more active than both microporous CsNaX and mesoporous OMS-NH₂.

The Knoevenagel condensation reactions on faujasite catalysts (i.e. NaY, NaX and CsNaX) are described by the reaction Scheme 1, where the catalyst activity is mainly due to the structural basicity of the zeolite. The negatively charged oxygen atoms of the zeolite framework exhibit Lewis base properties and the basicity of these sites depends on the framework counterion (e.g. Na⁺ and Cs⁺), the type and number of neighboring atoms and the chemical bond structure (i.e. bond length and angle). The recent review papers of Brunel et al. [29] and Weitkamp et al. [3] described how organic bases such as primary, secondary and tertiary amines can be attached to mesoporous silica surface by direct or post-synthesis silylation. Scheme 2 illustrates how the reaction between benzaldehyde and ethyl cyanoacetate is catalyzed by aminopropylated mesoporous silica (e.g. OMS-NH₂). The reaction is initiated when a benzaldehyde molecule reacts with a surface amine to form an imine compound. The addition of ethyl cyanoacetate and the subsequent molecular rearrangement produces the final reaction product and water molecule. In the reaction, the grafted organic amine acts as a Bronsted base.

Grafting organic amine molecules onto NaX and CsNaX zeolites does not only introduces new catalyst sites (i.e. Bronsted sites), but also perturbs the existing Lewis sites on the zeolites. The basicity of the grafted aminopropyl group is also affected by the substrate as shown by the reaction results in Fig. 3d. It can be deduced from the poor perfor-

mance of NaX-NH₂ for Knoevenagel condensation between benzaldehyde and diethyl malonate that the organic amines grafted onto NaX are weaker base compared to that attached to MCM-41 despite the higher reactivity of NaX-NH₂ for catalyzing the reaction between benzaldehyde and ethyl cyanoacetate. It is clear that the organic amines grafted onto CsNaX remains active for the reaction between benzaldehyde and DEM, and thus possess a stronger base property compared to the amines grafted onto MCM-41 and NaX. However, the exact chemical nature of the basic sites generated in CsNaX-NH₂ remained to be clarified.

3.2. Knoevenagel condensation reaction in microreactors

Fig. 4 displays the pictures of the multi-channel, membrane-catalyst plate after catalyst deposition and membrane growth. An estimated 0.005 g of zeolite catalyst powder (i.e. CsNaX and CsNaX-NH₂) was uniformly coated onto the microchannels. The catalyst particles were trapped on the grooves and crevices of the porous stainless steel (Fig. 4a). Powder adhesion was tested by flowing water-benzaldehyde solutions through the microchannels at 1 ml/h and 373 K for 20 h. Analysis of the reactor effluent at fixed intervals was unable to detect any dislodged particles. This clearly showed that there was a good catalyst adhesion on the microchannel. A 16 μm thick NaA membrane was grown on the back of the multi-channel plate. It can be seen from Fig. 4b that the membrane consists of well-intergrown NaA crystal grains. The stainless steel grains are completely clad with a layer of NaA zeolite film that also bridges the gaps formed between the sintered grains creating a defect free membrane (Fig. 4b, inset). This explains the superior membrane separation performance shown in Table 2. The

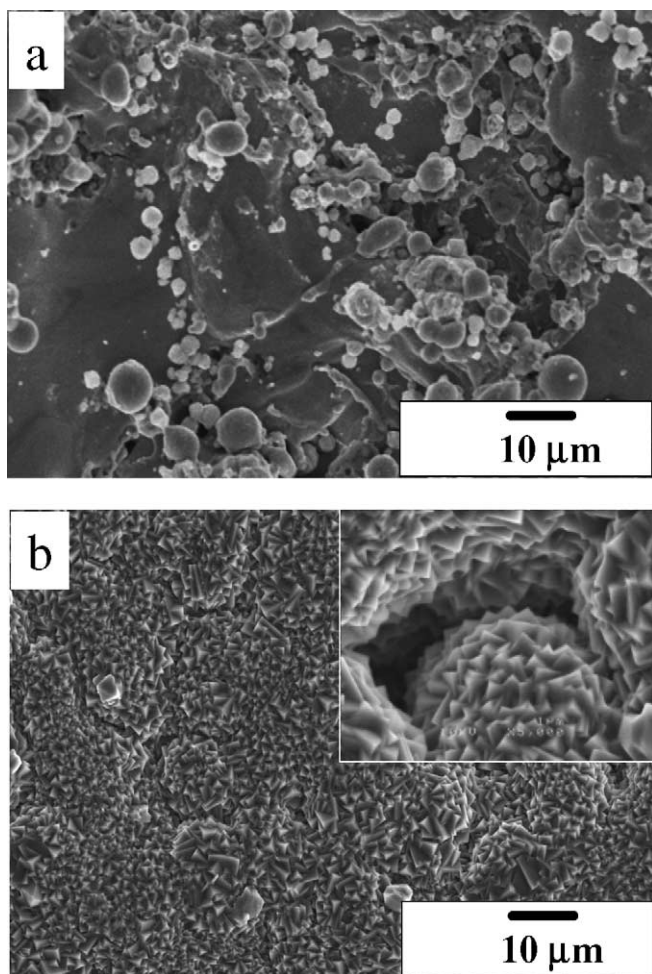


Fig. 4. Scanning electron microscope pictures of the multi-channel, membrane-catalyst plate showing (a) zeolite catalyst powder deposited in the microchannel and (b) NaA membrane grown on the porous stainless steel support.

table summarizes the results of the pervaporation experiments for different water-benzaldehyde mixtures. It can be seen from the data that the NaA membrane has an excellent selectivity for water even at high permeance.

Preliminary reaction studies were carried out using stoichiometric mixture of benzaldehyde and ethyl cyanoacetate on porous stainless steel substrate and zeolite membrane. The reaction temperature was set at 373 K and the flow rate

Table 2

Separation properties of NaA zeolite membrane deposited onto the multi-channel, membrane-catalyst plate for different water-benzaldehyde mixtures

| Water concentration (wt.%) | Permeation flux (P) ($\text{kg}^1 \text{m}^{-2} \text{h}^{-1}$) | Separation factor (α) |
|----------------------------|---|--------------------------------|
| 1 | 0.104 | 124,000 |
| 2 | 0.085 | 164,000 |
| 3 | 0.121 | 115,000 |
| 4 | 0.063 | 135,000 |
| 5 | 0.086 | 156,000 |

at 1 ml/h. No ethyl 2-cyano-3-phenylacrylate was produced from these experiments and only trace amount of benzoic acid was detected. This indicated that both stainless steel and zeolite materials were inert under the reaction conditions. Catalyst activation and deactivation can occur during the normal course of a reaction, but can be easily remedied by stabilizing the catalyst under the reaction conditions. The stabilized, catalyst-coated multi-channel membrane plate (CsNaX catalyst, NaA membrane) was monitored for more than 60 h under the reaction conditions. Except for an initial 5% lost in activity, both benzaldehyde conversion (20%) and ethyl 2-cyano-3-phenylacrylate yield (19.8%) were constant throughout the experiment. It is important to note that in order to establish the steady-state condition, effluent and permeate samples were collected at discrete intervals for analysis. Three measurements were made from each sample and the results were averaged. Material and carbon balances showed that the outlet streams added up to within 90% of the inlet value.

Fig. 5 compares the performance of the multi-channel microreactor to a traditional packed bed reactor (PBR). The laboratory-scale, tubular reactor has an i.d. of 6.5 mm and

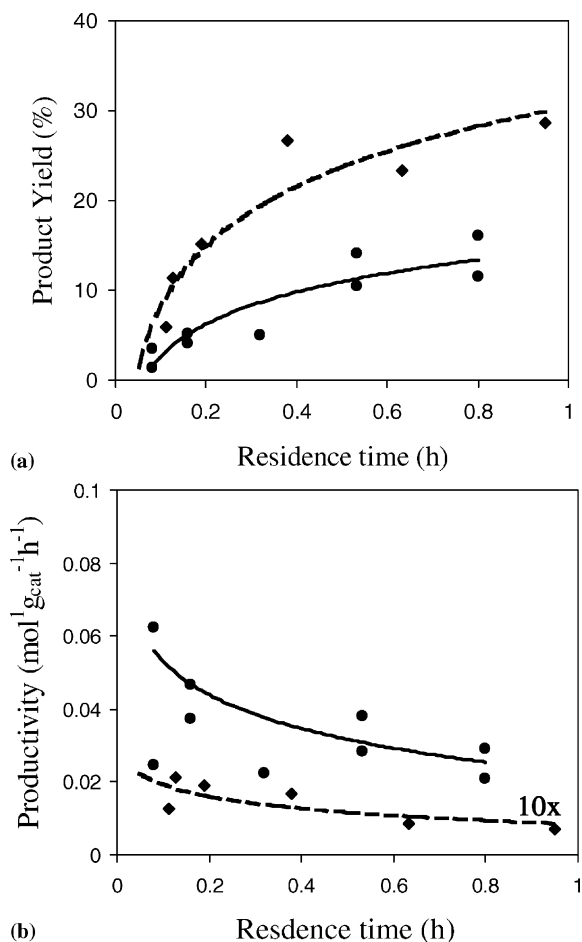


Fig. 5. Plots of (a) product yield and (b) productivity for the packed-bed reactor (\blacklozenge) and multi-channel reactor (\bullet) as a function of residence time. Please note the lines were drawn only to guide the eyes.

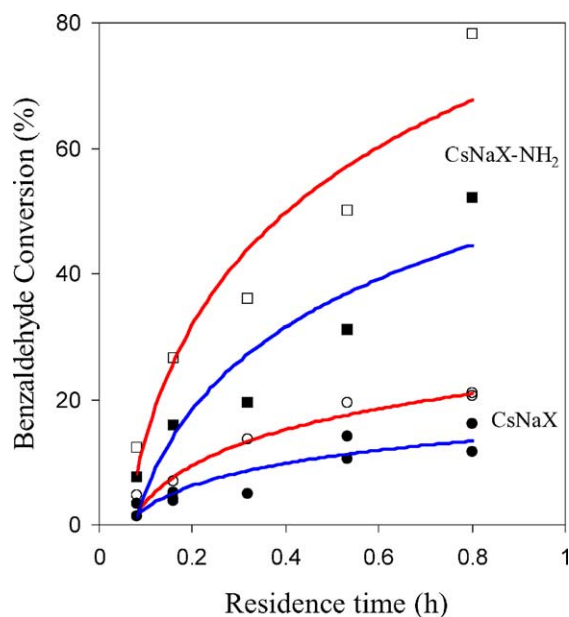


Fig. 6. Plots of benzaldehyde conversion as a function of residence time for microreactor and membrane microreactor using CsNaX (■, □) and CsNaX-NH₂ (●, ○) catalysts. Please note the closed and open symbols represent the microreactor and membrane microreactor data, respectively. Also, the lines were drawn only to guide the eyes.

a length of 75 mm giving the reactor a volume of 1.9 cm³. 3.6 g of CsNaX catalyst was needed to give the PBR a comparable level of reaction yield as the microreactor (Fig. 5a). The catalyst loading per unit reactor volume for the PBR was about 60 times (i.e. 1.9 g CsNaX per cm³ reactor) higher than the microreactor (0.03 g CsNaX per cm³ reactor). Thus, even though the yield of the PBR was higher than the microreactor, its productivity expressed in moles of ethyl 2-cyano-3-phenylacrylate produced per gram of catalyst per hour was significantly less than the microreactor (Fig. 5b). This can be attributed to the enhanced mass transfer rate in the microchannel as a result of a larger contact area and shorter diffusion path between the catalyst and reaction mixture. Both reactors produced only ethyl 2-cyano-3-phenylacrylate.

Faster reaction kinetics can further improve the performance of the microreactor. This can be achieved by either increasing the catalyst loading or improving the catalyst formulation. Indeed, the plots of benzaldehyde conversion versus residence time in Fig. 6 shows that substituting CsNaX-NH₂ catalyst for CsNaX resulted a nearly fourfold increase in reaction conversion. This is consistent with the kinetic data obtained from the batch reaction experiments. The Knoevenagel condensation reaction is constrained by unfavorable thermodynamic equilibrium. The continuous and selective removal of water from the reaction can lead to an increase in conversion for this equilibrium limited reaction [30]. Also, the water formed by the reaction can poison the zeolite catalyst, and its removal is a must if an optimum catalyst performance is to be expected. Fig. 6

shows that for both catalysts, the membrane microreactor outperformed the microreactor. A 25% improvement in conversion was obtained using the membrane microreactor. The conversion increases from 15 to 20% for the CsNaX catalyst and 55 to 80% for the CsNaX-NH₂. The removal of water has the added benefit of enhancing the product purity. Indeed, analysis of the permeate showed that only pure water was pervaporated across the zeolite membrane during the reaction, and calculations indicated that all water produced by the condensation reaction was completely removed by membrane pervaporation. It is clear that the membrane was operating below its capacity. This means that the performance of the membrane microreactor is limited mainly by the kinetics, now that both thermodynamic and mass transfer constraints were removed.

4. Concluding remarks

This work clearly demonstrated that new aminopropylated CsNaX outperformed both CsNaX and aminopropylated MCM-41 catalysts for the Knoevenagel condensation reaction between benzaldehyde and ethyl cyanoacetate, ethyl acetoacetate and diethyl malonate. The new catalyst was inexpensive, easy to prepare and stable. It maintained its original activity during a period of more than a year that constituted this study. Currently, experiments were underway to investigate the nature of the amino groups grafted onto the CsNaX-NH₂. This is expected to lead to more efficient catalysts. Besides catalyst improvement, reactor also plays an important role in chemical production. It is not uncommon to see labor intensive batch processes being used for the production of fine chemicals and pharmaceuticals instead of the more efficient continuous process. This usually results in significant waste generation during the scale-up from the laboratory to production scale. Microreactors offer an alternative way for the production of specialty chemicals and pharmaceuticals by a *continuous* process. Indeed, this study confirmed that microreactor could achieve better performance than a traditional packed-bed reactor. Also, the use of a membrane microreactor eliminated the thermodynamic constraint on the equilibrium-limited Knoevenagel condensation reaction resulting in higher product yield as well as better product purity. Microreactors also benefit from simpler process optimization, rapid design implementation, better safety and easier scale-up through replication enabling rapid product deployment to the marketplace and thus ensuring a significant competitive edge.

Acknowledgements

The authors would like to thank the Hong Kong Research Grant Council the Institute for Integrated Microsystems (I2MS-01/02.EG02) and the HKUST Postdoc Fellowship Matching Fund for funding this research. We thank Ms.

W.N. Lau for conducting the batch reaction experiments for OMS-NH₂ and for taking the SEM pictures of the multi-channel, membrane-catalyst plate. We also would like to acknowledge the Material Preparation and Characterization Facility (MCPF) of Hong Kong University of Science and Technology.

References

- [1] H. Hattori, Chem. Rev. 95 (1995) 537.
- [2] D. Barthomeuf, Catal. Rev. 38 (1996) 521.
- [3] J. Weitkamp, M. Hunger, U. Ryma, Microporous Mesoporous Mater. 48 (2001) 255.
- [4] A. Corma, S. Iborra, S. Miguel, J. Primo, J. Catal. 173 (1998) 315.
- [5] C. Moreau, R. Durand, A. Rous, D. Tichit, Appl. Catal. A: Gen. 193 (2000) 257.
- [6] A. Corma, R.M. Martin-Aranda, F. Sanchez, J. Catal. 126 (1990) 192.
- [7] A. Corma, R.M. Martin-Aranda, Appl. Catal. A: Gen. 105 (1993) 271.
- [8] K.R. Kloetstra, H. van Bekkum, Stud. Surf. Sci. Catal. 105A (1997) 431.
- [9] K.R. Kloetstra, J. van den Broek, H. van Bekkum, Catal. Lett. 47 (1997) 235.
- [10] G.T. Kerr, G.F. Shipman, J. Phys. Chem. 72 (1968) 3071.
- [11] Y.S.S. Wan, J.L.H. Chau, A. Gavriilidis, K.L. Yeung, Microporous Mesoporous Mater. 42 (2001) 157.
- [12] E.V. Rebrov, G.B.F. Seijger, H.P.A. Calis, M.H.J.M. de Croon, C.M. van den Bleek, J.C. Schouten, Appl. Catal. A 206 (2001) 125.
- [13] Y.S.S. Wan, A. Gavriilidis, J.L.H. Chau, K.L. Yeung, Chem. Commun. 8 (2002) 878.
- [14] J.L.H. Chau, A.Y.L. Leung, K.L. Yeung, Lab-on-a-Chip 3 (2003) 53.
- [15] J.L.H. Chau, Y.S.S. Wan, A. Gavriilidis, K.L. Yeung, Chem. Eng. J. 88 (2002) 187–200.
- [16] J.L.H. Chau, K.L. Yeung, Chem. Commun. 9 (2002) 960.
- [17] A. Gavriilidis, P. Angeli, E. Cao, K.K. Yeong, Y.S.S. Wan, Trans. IChemE 80 (2002) 3.
- [18] Y.S.S. Wan, A. Gavriilidis, K.L. Yeung, Trans. IChemE 81 (2003) 753.
- [19] S.M. Lai, R. Martin-Aranda, K.L. Yeung, Chem. Commun. 2 (2003) 218.
- [20] J.L.H. Chau, A.Y.L. Leung, M.B. Shing, K.L. Yeung, C.M. Chan, in: Z. Tang, P. Sheng (Eds.), Nano Science and Technology: Novel Structure and Phenomena, Taylor and Francis, London, 2003, pp. 228–232.
- [21] M.M.J. Treacy, J.B. Higgins, R. Ballmoos, Collection of Simulated XRD Powder Patterns for Zeolites, Elsevier, New York, 1996, pp. 446–447 and 524–525.
- [22] C.E.A. Kirschhock, B. Hunger, J. Martens, P.A. Jacob, J. Phys. Chem. B 104 (2000) 439.
- [23] I. Rodriguez, H. Cambo, D. Brunel, M. Lasperas, P. Geneste, Stud. Surf. Sci. Catal. 78 (1993) 623.
- [24] M. Lasperas, H. Cambo, D. Brunel, I. Rodriguez, P. Geneste, Microporous Mater. 7 (1996) 61.
- [25] U. Ryma, M. Hunger, H. Knozinger, J. Weitkamp, Stud. Surf. Sci. Catal. 125 (1999) 197.
- [26] M. Laspéras, T. Llorett, L. Chaves, I. Rodriguez, A. Cauvel, D. Brunel, Stud. Surf. Sci. Catal. 108 (1997) 75.
- [27] A. Corma, R.M. Martin-Aranda, V. Fornés, J. Primo, H. Garcia, Appl. Catal. A: Gen. 95 (1990) 237.
- [28] K.Y. Ho, G. McKay, K.L. Yeung, Langmuir 19 (2003) 3019.
- [29] D. Brunel, A.C. Blanc, A. Galarnéau, F. Fajula, Catal. Today 73 (2002) 139.
- [30] J.G.S. Marciano, T.T. Tsotsis, Catalytic Membranes and Membrane Reactors, Wiley-VCH, Weinheim, 2002, pp. 97–132.